Angewandte Chemie
Eine Zeitschrift der Gesellschaft Deutscher Chemiker

Supporting Information

69451 Weinheim, Germany

Controlling an Electron-Transfer Reaction at a Metal Surface by Manipulating Reactant Motion and Orientation**

*Nils Bartels, Bastian C. Krüger, Daniel J. Auerbach, Alec M. Wodtke, and Tim Schäfer**

anie_201407051_sm_miscellaneous_information.pdf

Supporting information

Experimental Section

Experiments are carried out in a molecular beam scattering apparatus described previously.[1] A pulsed molecular beam of cold NO molecules (TROT ≈ 6 K) is produced by expanding mixtures of NO seeded in a carrier gas into the vacuum through a piezoelectric valve (1 mm Ø nozzle, 10 Hz, 3 atm stagnation pressure).
After passing a 2 mm electro-formed skimmer (Ni Model 2, Beam dynamics, Inc.) 3 cm downstream, the beam enters a differentially pumped region. Here, molecules are prepared in the rotational ground state (J=0.5) of a highly excited vibrational state (vI=16 or vI=11) of the electronic ground state (X 2Π1/2) using the Pump-Dump-Sweep method and the same laser systems and optical transitions as described earlier.[2] The preparation is monitored by laser-induced fluorescence (LIF) and fluorescence depletion spectroscopy using a quartz lens and a photomultiplier tube (PMT, Hamamatsu, R7154). Subsequently, the prepared molecules enter another differentially pumped chamber through a pinhole and scatter from a clean Au(111) surface under ultra-high vacuum conditions. Before measurements are carried out, the Au(111) crystal is cleaned by sputtering with an Ar-ion gun (LK Technologies; NGI3000). The surface is then annealed for 20 min at 950 K, and surface cleanliness is verified with Auger electron spectroscopy. The UV light used for REMPI detection is the output of a frequency-doubled visible commercial OPO system (Continuum Sunlite Ex; 3-GHz bandwidth; 2 mJ/pulse at 250 nm). The detection takes place close to the surface and with a large beam diameter that collects molecules scattered over all possible scattering angles. The electric field strengths for the orientation experiments were 30 kV/cm for both polarities.

Data Analysis

Prior to scattering, molecules are prepared in the rotational ground state (J=0.5, Ω=0.5) of a high vibrational state v_I=11 or 16 by an approach called Pump-Dump and Sweep. This technique uses three different laser pulses (Pump-Dump and Sweep) to achieve high quantum state purity in the incident molecular beam and was described in detail in a previous publication.[S2] After scattering from the Au(111) surface the density of states is distributed over many ro-vibrational states. This leads to congested resonance enhanced multi-photon ionization (REMPI) spectra, which we analyze in order to derive vibrational state distributions.
In order to obtain information about all possible scattering channels we measure REMPI spectra over a wide range of wavelengths (235 nm to 315 nm for v_I=11 and 245 nm to 350 nm for v_I=16). An example is shown in Figure S1-A. Spectra are corrected for the photon density (which means they are divided by the laser pulse energy and the wavelength). Resonant ionization is achieved with a commercially available optical parametric oscillator laser system (Continuum Sunlite EX OPO with FX1 frequency conversion unit). Spectra are recorded in steps of 5 to 10 nm and after each scan a background spectrum (with blocked Dump pulse) is recorded. At the used laser powers (~1 mJ/pulse with 3 mm beam diameter) most of the REMPI signal results from ionization via the A $^2\Sigma^+$ state of NO.

By analyzing the intensity of non-overlapping single REMPI lines we obtain rotational state distributions for several vibrational states. An example of a rotational state distribution of molecules prepared in v_I=11 and scattered back in v=9 is shown in Figure S1-B. The rotational state distributions are different depending mostly on the incidence kinetic energy, but also on the incidence orientation as well as incident and final and vibrational states. In general, rotational state distributions are non-thermal and exhibit strong rotational rainbows. We will discuss this issue in more detail in a future publication.

With the rotational state distributions derived in this way, it is then possible to obtain a fit of the entire REMPI spectra (Fig S1-C). We fit the substracted spectrum (Signal minus background as shown in Figure S1-A). To speed up the fitting procedure, spectra are binned in intervals of 1 cm^{-1}. In the fit, the rotational state distributions are assumed to be independent of the final vibrational state at a given incidence translational energy.
As a result of the fitting procedure we obtain intensities for the different REMPI bands (see Figure S1-D). The different symbols in the figure describe which vibrational state of A $^2\Sigma^+$ is used for ionization. Most vibrational states are probed via different ionization channels.

For most vibronic bands in the A-X system of NO we saturated the first step of the resonant ionization by the probe laser, so that no correction for varying Franck-Condon factors in the detection step is needed. Instead, we verified the

vibrational-state-specific detection efficiencies for each band experimentally. For this, we prepared controlled vibrational population distributions of highly vibrationally excited NO via spontaneous emission from laser-prepared vibrational levels of the B $^2\Pi_{1/2}$ state of NO. In case of strong deviations between the expected and observed intensity of a particular REMPI band, it was not included in the following analysis (Figure S1-E). This way we make sure not only to avoid relying on absorption bands being only partially saturated, but also avoid problems such as pre-dissociation, which might otherwise falsify the final vibrational state distributions.

The final vibrational state distributions are then obtained by averaging the corrected band intensities for each vibrational state (see Figure S1-F). Within this step we also apply a density-to-flux conversion. For the case of scattering NO(v_I=3) from Au(111) velocities of scattered molecules have been measured extensively and it was found that the final velocities are coupled to the rotational excitation and also weakly coupled to vibrational energy loss.[3] We assume that NO (v_I=16, 11) scattering exhibits a very similar translational-rotational and translational-vibrational coupling as NO (v_I=3) and extrapolate the unknown velocities from the data of v_I=3. The effect of the density-to-flux conversion on the population of a final vibrational state is always smaller than 20 %.

An entire REMPI spectrum and its simulation are shown in Figure S2 for the case of NO (v_I=16) with an incidence translational energy of 0.52 eV. Good agreement between spectrum and simulation is achieved.

Potential energy curves

In order to qualitatively compare experimental observations we have estimated potential energy curves for neutral NO and its anion both with a fixed bond length approaching the Au(111) surface. Since the probability density of a highly vibrationally excited molecule has its maximum near the classical outer turning point of the vibration, the corresponding bond length is used in the calculations. Hence, a bond length of 1.59 Å corresponds to a molecule in the vibrational state v=16 (1.48 Å corresponds to v=11, 1.30 Å corresponds to v=3). The plotted neutral potentials use the potential and parameters for the NO-Ag(111) interaction as given in references.[S4a, S4b] The potential is modified to agree with the calculation of the position of the potential energy well for NO approaching a Au(111) surface at an hexagonal close-packed hollow site (1.82 Å, reported in reference [S5]). The neutral potentials shown represent an approach of NO to this site.

The interaction of the anionic species with the surface is approximated by Coulombic forces between the anion´s charge and the image charge on the metal surface resulting in an image potential[6]

$$U_{\text{image}} = \frac{e^2}{4\pi\varepsilon_0 4(z-d+s)},$$

where z is the distance of the center of mass of NO from the surface and d=0.6 Å taken from reference [S7]. The parameter s takes into account that the charge of the anion might not be evenly distributed across the molecule. Roughly, the position of the charge on the anion is approximated as the center of charges between two partial charges located at the positions of the atoms. The partial charge´s fraction in terms of the total charge is assumed to be equivalent with the contribution of the atom´s orbitals to the LUMO of NO as calculated by density functional theory (a=30 % of the charge is located at the O-atom[S8]). Thus, at the same molecule center of mass-surface distance an orientation of the O-atom towards the surface results in a larger distance of the position of the negative charge and the surface compared to the reverse orientation of NO. The parameter s is calculated via the equation:

$$s = R_{\text{NO}}\cos(\theta)(1 - a - m_{\text{O}}\,(m_{\text{O}} + m_{\text{N}})^{-1}).$$

Here m_N (m_O) is the mass of nitrogen (oxygen) and θ is the angle between the surface normal and a vector pointing from the O-atom towards the N-atom of the molecule. The anionic potentials shown represent approaches of NO towards the surface with different angles $\theta = 90°; 68°; 112°$. An angle of 90° corresponds to a side-on collision. An angle of 68° (O-atom first, positive charge at the electrode used for orientation), respectively 112° (N-atom first, negative charge at the electrode) corresponds to $\langle\theta_{max}\rangle$ achieved in the experiment when an electric orientation field is applied.

The difference of anion and neutral in potential energy at infinite distance from the surface is derived by the difference of the work function of the surface (5.31 eV) minus the vertical electron binding energy of NO at the given bond length (see also reference [S9]).

In Figure 4 in the main article we show only the orientation dependence of the anionic potential energy curves. Please note that the neutral curves also show an orientation dependence which is much weaker than for the ionic curves, and are thus omitted from Figure 4 for clarity. Figure S3 shows corresponding curves, where the orientation dependence of both neutral and anionic curves are displayed. It is obvious that the orientation dependence of the neutral curve is small at the distances where curve crossing occurs.

Figures

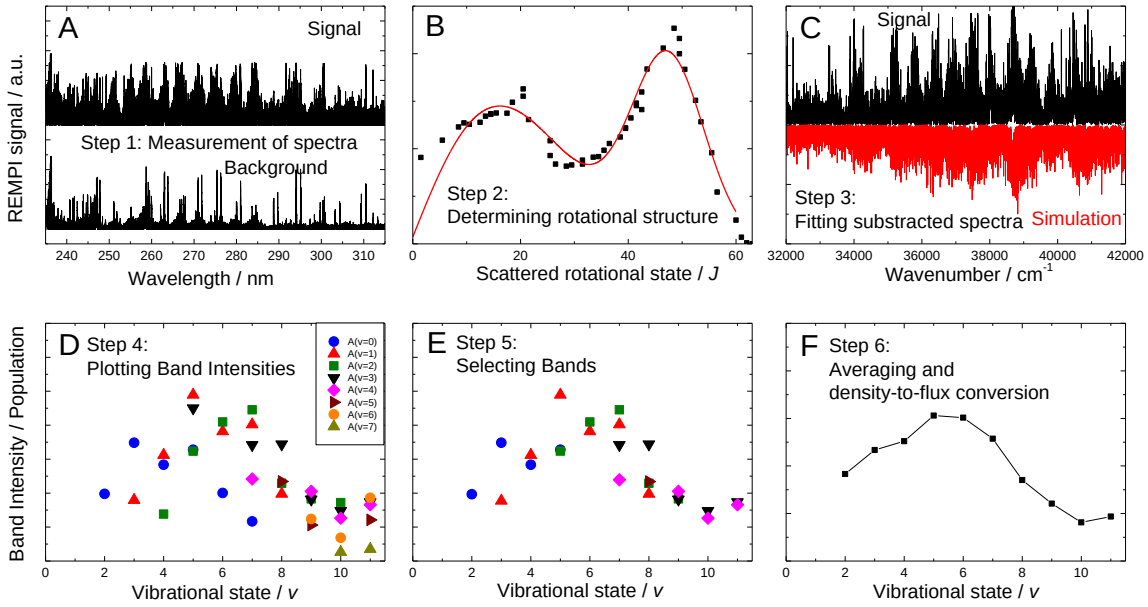

Figure S1. Steps in the data analysis for determining vibrational state distributions. The panels are explained in the text. The data shown belongs to a measurement for v_I=11 at an incidence translational energy of 0.51 eV.

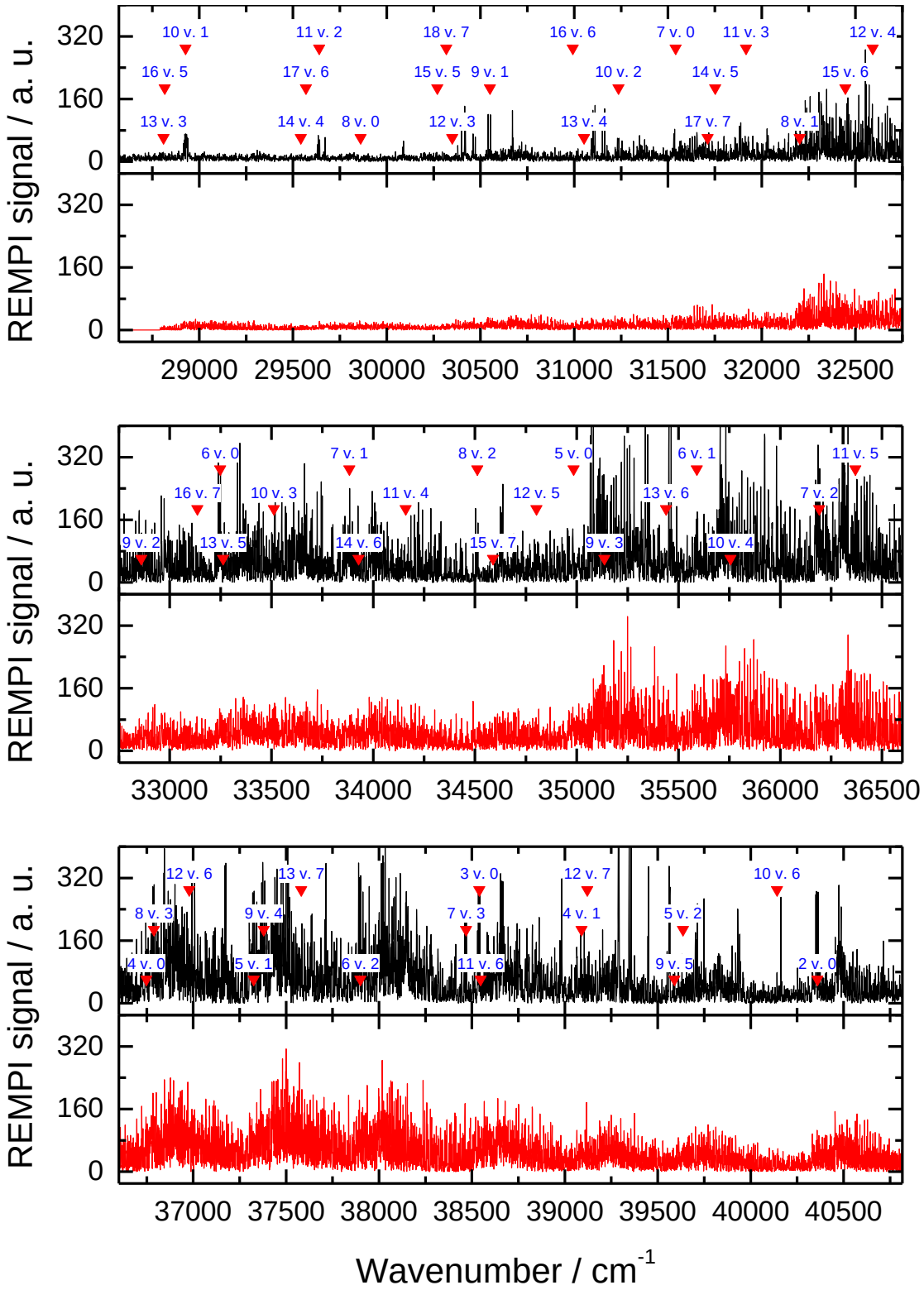

Figure S2. Comparison of a measured REMPI spectrum (top panels, black) and a simulation (bottom panels, red). Both the REMPI spectrum and the simulation are binned in intervals of 1 cm^{-1}. In the example, NO molecules are initially prepared in v_I=16 at an incidence translational energy of 0.52 eV. The REMPI signal is divided by the number of photons in the pulse of the probe laser. The red triangles describe the position of the $R_{11}(0.5)$ transitions for the REMPI bands described by the blue label. As an example the label "2 v.0" indicates that molecules in v=2 of the electronic ground state are ionized via the v=0 state of A $^2\Sigma^+$.

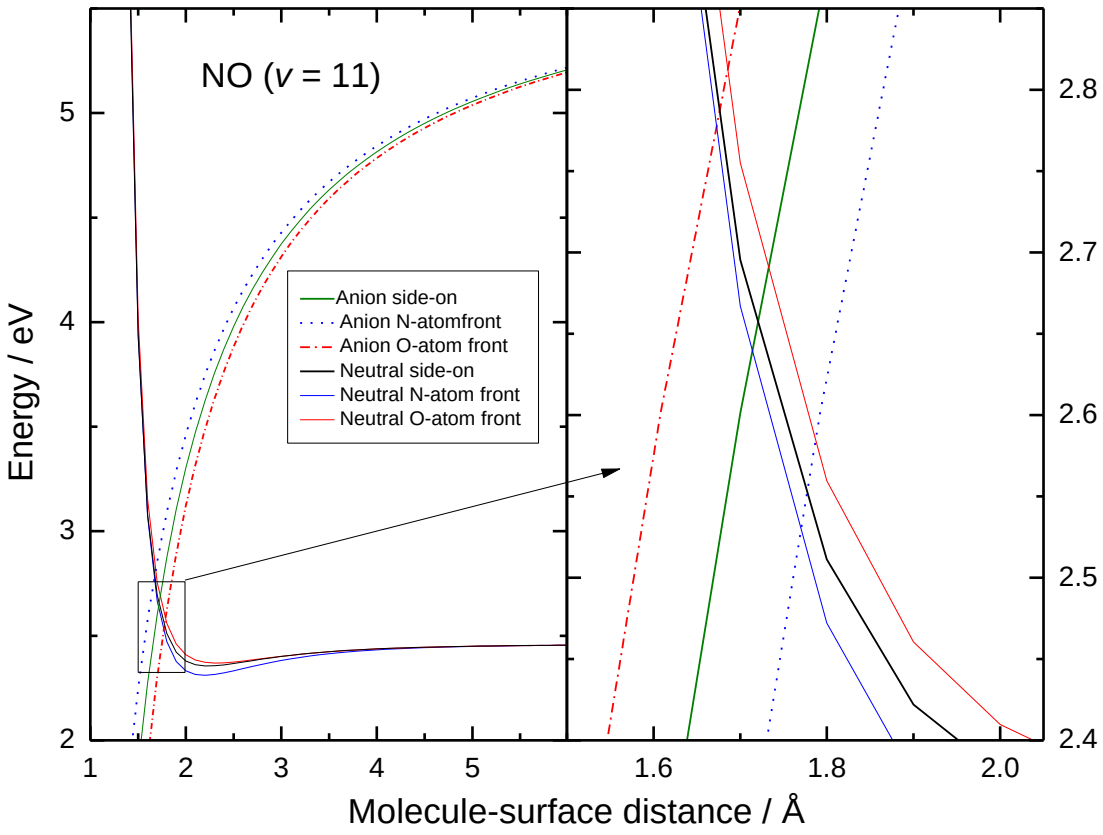

Figure S3. *Potential energy curves of neutral and anionic NO for N-front, O-front and side on collisions. It is obvious that the orientation effect is much stronger for the anionic curves than for the neutral curves.*

References

[1] J. Chen, D. Matsiev, J. D. White, M. Murphy, A. M. Wodtke, *Chemical Physics* **2004**, *301*, 161-172.

[2] N. Bartels, B. C. Krüger, S. Meyer, A. M. Wodtke, T. Schäfer, *Journal of Physical Chemistry Letters* **2013**, *4*, 2367-2370.

[3] K. Golibrzuch, P. R. Shirhatti, J. Altschäffel, I. Rahinov, D. J. Auerbach, A. M. Wodtke, C. Bartels, *Journal of Physical Chemistry A* **2013**, *117*, 8750-8760.

[4] (a) C. W. Muhlhausen, L. R. Williams, J. C. Tully, *Journal of Chemical Physics* **1985**, *83*, 2594-2606; (b) J. Kimman, C. Rettner, D. Auerbach, J. Barker, J. Tully, *Physical Review Letters* **1986**, *57*, 2053-2056.

[5] S. Roy, N. A. Shenvi, J. C. Tully, *The Journal of Chemical Physics* **2009**, *130*, 174716.

[6] J. A. Appelbaum, D. R. Hamann, *Physical Review B* **1972**, *6*, 1122-1130.

[7] Y. Harada, S. Masuda, H. Ozaki, *Chem Rev* **1997**, *97*, 1897-1952.

[8] A. J. Komrowski, H. k. Ternow, B. Razaznejad, B. Berenbak, J. Z. Sexton, I. Zoric, B. Kasemo, B. I. Lundqvist, S. Stolte, A. W. Kleyn, A. C. Kummel, *The Journal of Chemical Physics* **2002**, *117*, 8185-8189.

[9] J. D. White, J. Chen, D. Matsiev, D. J. Auerbach, A. M. Wodtke, *Journal of Chemical Physics* **2006**, *124*, 064702.